Advances in Geo-Energy Research

Vol. 18, No. 3, p. 272-286, 2025

Original article

Novel encapsulated surfactants for enhanced oil recovery in carbonate reservoir conditions: Interfacial and wetting behavior

Arsenii Chekalov[1], Anastasia Ivanova[1], Alexey Sokolov[2], Gleb Sukhorukov[2,3], Alexey Cheremisin[1], Chengdong Yuan[1]*

[1]*Center for Petroleum Science and Engineering, Skolkovo Institute of Science and Technology, Moscow 121205, Russia*

[2]*Vladimir Zelman Center for Neurobiology and Brain Rehabilitation, Skolkovo Institute of Science and Technology, Moscow 121205, Russia*

[3]*School of Engineering and Materials Science, Queen Mary University of London, London E1 4LJ, United Kingdom*

Keywords:
Enhanced oil recovery
surfactant
encapsulation
nanocarriers
interfacial tension

Cited as:
Chekalov, A., Ivanova, A., Sokolov, A., Sukhorukov, G., Cheremisin, A., Yuan, C. Novel encapsulated surfactants for enhanced oil recovery in carbonate reservoir conditions: Interfacial and wetting behavior. Advances in Geo-Energy Research, 2025, 18(3): 272-286.
https://doi.org/10.46690/ager.2025.12.06

Abstract:
Surfactant encapsulation presents a novel strategy for the targeted delivery of active molecules to oil reservoirs. This study investigates the interfacial tension, wettability alteration, static adsorption and oil displacement performance of two novel encapsulated surfactants, anionic alkyl ether carboxylate and non-ionic alkyl polyglucoside, in water-oil and water-oil-carbonate rock systems. A refined synthesis yielded silica carriers with dimensions appropriate for transport through carbonate reservoir pore networks, preventing pore blockage while enabling effective delivery. A synergism between the surfactants and silica nanoparticles, released upon carrier rupture, was confirmed. The cooperative action of silica nanoparticles and surfactant molecules, facilitated by multiple intermolecular forces, including hydrogen bonding, electrostatic, and hydrophobic, enhanced the efficiency of interfacial adsorption, leading to a significant reduction in interfacial tension compared to pure surfactant systems. Furthermore, silica nanoparticles accelerated the alteration in wettability towards a hydrophilic state via disjoining pressure and competitive adsorption on the carbonate surface. Consequently, the simultaneous enhancement of interfacial behavior and mitigation of static adsorption due to encapsulation translated into more efficient oil displacement compared to use of the pure surfactants. This work demonstrates that encapsulation not only reduces adsorption but also enhances interfacial performance and displacement efficiency, supporting its potential application in chemical enhanced oil recovery.

1. Introduction

Surfactant flooding constitutes a prominent chemical enhanced oil recovery (EOR) technique for mobilizing residual oil. The efficacy of surfactants stems from their capacity to drastically reduce oil-water interfacial tension (IFT), alter reservoir wettability, and generate stable foams, rendering them applicable across diverse reservoir types (Lv et al., 2023). A principal impediment to this process is the significant adsorption of surfactant molecules onto reservoir rock surfaces. This phenomenon, characterized by the accumulation of species at the solid-liquid interface, results in substantial surfactant loss before reaching the target oil bank. The primary mechanisms governing surfactant adsorption include electrostatic interactions (e.g., ion exchange, ion pairing), hydrogen bonding, and van der Waals forces (Zhang and Somasundaran, 2006; Liu et al., 2021b) . The extent of adsorption is governed by critical factors such as surfactant charge, rock mineralogy, brine salinity, pH, and temperature (Mushtaq et al., 2015; Saha et al., 2017; Belhaj et al., 2020b). This

Yandy Scientific Press

*Corresponding author.
E-mail address: Arsenii.Chekalov@skoltech.ru (A. Chekalov); Anastasia.Ivanova@skoltech.ru (A. Ivanova); Alexey.Sokolov@skoltech.ru (A. Sokolov); G.Sukhorukov@skoltech.ru (G. Sukhorukov); A.Cheremisin@skoltech.ru (A. Cheremisin).

Received October 18, 2025; revised November 13, 2025; accepted November 29, 2025; available online December 4, 2025.

loss not only diminishes process efficiency but also escalates operational economics due to the need for larger chemical inventories.

A conventional strategy to mitigate adsorption involves the introduction of sacrificial agents. Compounds such as polyelectrolytes, nanoparticles, alkalis, and polymers have been explored for this role (Zhang et al., 2009; Yekeen et al., 2017; Wang et al., 2022). For instance, anionic polyacrylates can pre-adsorb onto surfaces, competitively excluding subsequent anionic surfactant adsorption (ShamsiJazeyi et al., 2013; Liu et al., 2021a). Nanoparticles may function by sterically blocking adsorption sites or, through mechanical action, displacing adsorbed surfactant molecules (Suresh et al., 2018), Alkalis like sodium hydroxide (NaOH) and sodium carbonate (Na_2CO_3) can induce a more negative surface charge on sandstones (at pH > pHpzc), generating electrostatic repulsion against anionic surfactant headgroups (Zhou et al., 2005; Olajire, 2014; Wu et al., 2017). However, their incompatibility with divalent ions (e.g., Ca^{2+}, Mg^{2+}), leading to damaging precipitates, limits their utility in carbonate formations (Chang et al., 2018). Alternative alkalis such as ammonium hydroxide (NH_4OH) and sodium metaborate ($NaBO_2$) have been proposed, though issues of cost and lack of universality restrict widespread field application (Falcone et al., 1982; Zhang et al., 2009; Sharma et al., 2015).

An emerging alternative is the encapsulation of surfactants within protective carriers. This approach aims to minimize adsorption losses through targeted delivery and release triggered by specific reservoir conditions (e.g., elevated temperature, salinity, or contact with oil), thereby enhancing the concentration of active molecules at the displacement front. Previous studies have demonstrated the promise of this concept. Alhassawi and Romero-Zeron reported a 64%-76% reduction in static adsorption for sodium dodecyl sulfate encapsulated in β-cyclodextrin, with concomitant improvements in oil recovery (Alhassawi and Romero-Zerón, 2015a, 2015b, 2015c). Rosestolato et al. (2019) achieved a high loading capacity (96%) of a nonionic surfactant in beeswax nanoparticles, noting IFT performance comparable to the pure surfactant, albeit in simple NaCl brine without wettability assessment. Nevertheless, as a low-melting organic carrier, beeswax is less suitable for maintaining delivery efficiency at elevated temperatures and in mineralogically complex formations, where particle retention and surfactant losses may still occur. Cortés et al. (2018) documented a 100-fold reduction in IFT using resin-shell nanocarrier and emphasized the necessity for evaluation under reservoir conditions, but these nanocapsules have so far only been tested in sandstone micromodels at near-ambient conditions, and their thermal stability and retention under realistic reservoir conditions remain to be demonstrated. Ojo et al. (2020) and Yu et al. (2021) developed encapsulated systems (using ethyl cellulose and wax-coated halloysite nanotubes, respectively) that demonstrated excellent stability under harsh conditions and provided superior oil recovery compared to surfactant alone. However, both approaches rely on rapid, interface-triggered release of surfactants, which offers limited flexibility for tuning release rate or adapting the delivery profile for various reservoir conditions.

In the context of abovementioned limitations of different surfactant carriers, silica-based carriers are particularly attractive due to their inorganic rigidity, excellent chemical and thermal stability, adjustable size in the sub-100 nm range and the possibility to tailor shell porosity and surface chemistry to control both surfactant release and rock-fluid interactions. Alsmaeil et al. (2021) described a new hollow silica-based platform for surfactant delivery with high effectiveness in IFT reduction and wettability alteration. While this study elegantly demonstrates slow surfactant release and wettability alteration on model glass/oil systems, its applicability under realistic reservoir conditions (carbonate rock, crude oil, and long-distance transport in porous media) remains largely untested. Ahsaei et al. (2024) developed a nanocomposite capsule based on mesoporous silica functionalized with thermosensitive poly(N-vinylcaprolactam), aimed at achieving controlled release under elevated reservoir temperatures. However, a noticeable portion of the surfactant was released already at room temperature and in distilled water, suggesting insufficient thermal gating and limiting direct field applicability. In a subsequent study, the same group showed that loading cetyltrimethylammonium bromide into these capsules could enhance the overall interfacial performance of the formulation (Ahsaei et al., 2025), although the issue of premature release remains to be addressed for carbonate reservoir deployment. In the previous work, three surfactants (sodium dodecyl sulfate, alpha-olefin sulfonate, and cetrimonium bromide) were successfully encapsulated in 176-313 nm capsules and reduced adsorption and delayed release were reported (Ivanova et al., 2024).

In carbonate reservoirs, nonionic and mixed-type surfactants such as alkyl ether carboxylates (AEC) and alkyl polyglucosides (APG) have recently attracted significant attention due to their high salinity tolerance and environmental (Alvarez Jürgenson et al., 2015; Belhaj et al., 2020a; Tripathi et al., 2024). In spite of this fact, significant adsorption remains a major obstacle to their deep propagation and efficient field deployment (Wei et al., 2020). Scerbacova et al. (2023) confirmed that AEC surfactants can reach adsorption levels of up to $\sim$ 10 mg per gram of carbonate rock, and highlighted the critical influence of brine salinity on the magnitude of this retention.

The present study investigates interfacial behavior of two novel encapsulated surfactants: An anionic-nonionic AEC and a non-ionic APG. A refined synthesis yielding sub-150 nm carriers is reported and a detailed comparative analysis of the IFT reduction, wettability alteration, adsorption reduction and oil recovery efficiency of pure versus encapsulated surfactants under reservoir-like conditions is presented.

2. Materials and methods

2.1 Materials

The anionic-nonionic surfactant AEC (98% active content) and the nonionic surfactant APG (52% active content) were employed in this study. Tetraethyl orthosilicate (TEOS) and 3-aminopropyl-triethoxysilane (APTES), procured from Sigma-Aldrich, were used as received without further purification.

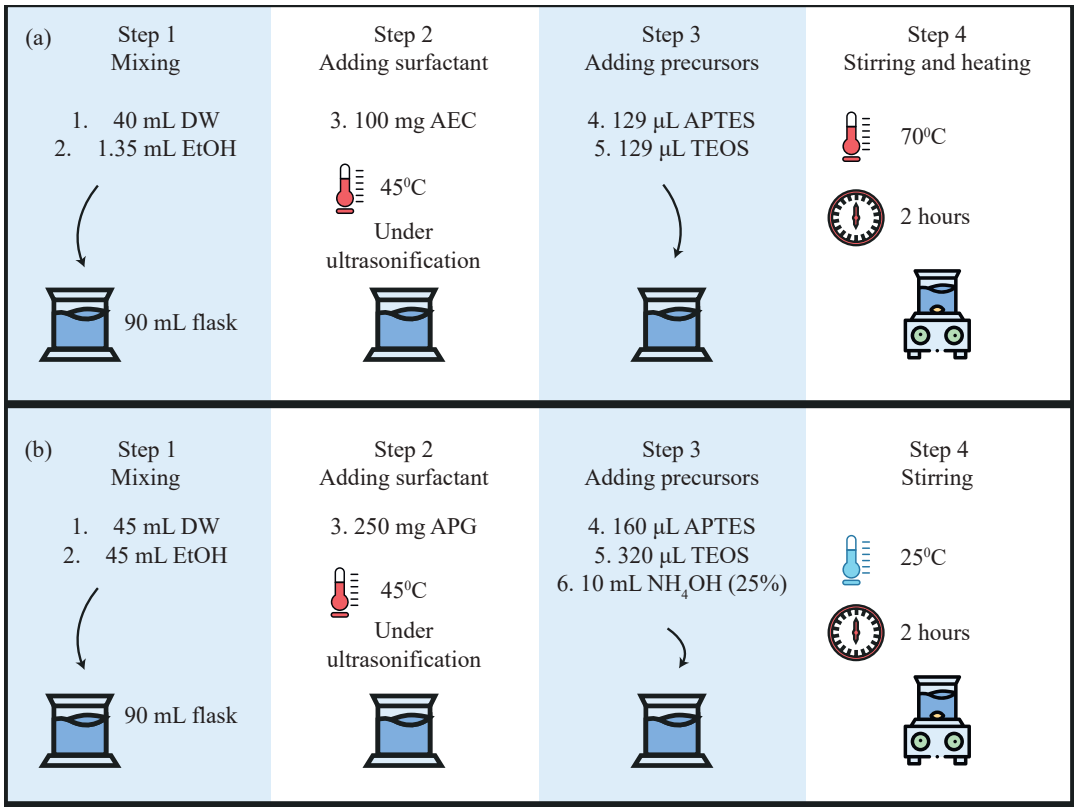

Fig. 1. Synthesis process of (a) AEC and (b) APG carriers.

The critical micelle concentration (CMC) values of surfactants were obtained from literature as 0.025%-0.05% for AEC and 0.015%-0.05% for APG (Scerbacova et al., 2023; Zhang et al., 2025). Aqueous brine solutions were prepared using deionized water and analytical-grade salts: 85% sodium chloride (NaCl), 7.5% calcium chloride dihydrate ($CaCl_2 \cdot 2H_2O$), and 7.5% magnesium chloride hexahydrate ($MgCl_2 \cdot 6H_2O$). Oil and rock samples are from an oil-saturated carbonate formation in Western Siberia. The crude oil had a measured density of 0.89 g/mL at 25 °C and 0.85 g/mL at 70 °C, with a water content of less than 1 wt%. The core cylinders (35 mm diameter × 30 mm length) were drilled from the reservoir formation. X-ray diffraction analysis was performed using a Huber G670 diffractometer (Huber Diffraktionstechnik GmbH, Germany), confirming that the rock substrate was predominantly calcite (≈ 99%).

2.2 Synthesis and characterization

2.2.1 Synthesis of silica nanocarriers

Surfactant-loaded silica nanoparticles (SNPs) were synthesized via a sol-gel process (Alsmaeil et al., 2021; Ivanova et al., 2024). For the encapsulation of AEC, a solution was prepared by combining deionized water (40 mL) and absolute ethanol (1.35 mL) in a 90 mL volumetric flask. AEC surfactant (100 mg) was dissolved in the solvent mixture under ultrasonication at 45 °C and added to the flask. Subsequently, 129 µL of APTES and 129 µL of TEOS were added as silica precursors. The reaction mixture was then heated to 70 °C and stirred at 500 rpm for 2 h. The synthesis scheme is illustrated in Fig. 1. For the encapsulation of APG, 45 mL of water and 45 mL of ethanol were mixed. 250 mg of APG surfactant was dissolved into the solvent mixture under ultrasonication at 45 °C and added into the flask. Subsequently, 160 µL of APTES and 320 µL of TEOS were added as silica precursors. 10 mL of NH_4OH solution (25%) was added to the mixture, followed by 2 h of mixing at room temperature.

2.2.2 Nanocarrier characterization

The hydrodynamic diameter and zeta potential of the synthesized nanocarriers were determined by dynamic light scattering using a Zetasizer Nano ZS instrument (Malvern Panalytical, United Kingdom). Each sample was diluted with deionized water and sonicated for 1 min to ensure proper dispersion. The resulting suspension (1 mL) was then transferred into a U-shaped capillary cell and allowed to equilibrate for 5 min at 298 K prior to measurement. Morphological characterization was performed by scanning electron microscope (SEM) Quattro S (Thermo Fisher Scientific, USA). Fourier transform infrared spectroscopy (FTIR) analysis was performed using a Bruker Tensor 27 spectrometer (Bruker Optics, Germany) in attenuated total reflectance mode to assess the chemical composition of the synthesized nanocarriers.

2.3 IFT measurements

IFT measurements at the oil-water interface were performed using the spinning drop tensiometer (Krüss GmbH, Germany) at a rotation speed of 6,000 RPM. Experiments were conducted at 25 and 70 °C, to assess thermal stability and

performance under reservoir-relevant conditions. The profile of the rotating oil droplet was analyzed by fitting the Young-Laplace equation using the instrument's proprietary software (Krüss Advance). The reported IFT value for each sample represents the mean of three independent measurements. The criterion for equilibrium was defined as a change in the measured IFT of less than 5% over a consecutive 15-minute interval. Measurements were recorded only after this stable condition was achieved. The selection of surfactant concentrations follows a unified design strategy. IFT measurements were conducted across sub-CMC, near-CMC and post-CMC regimes to determine optimal interfacial activity. Based on these findings, post-CMC concentrations were used further in the wettability, static adsorption and oil recovery factor (ORF) experiments, as these conditions best reflect practical EOR formulations.

2.4 Wettability measurements

The efficacy of both pure and encapsulated surfactant solutions in altering the wettability of carbonate rock from hydrophobic to hydrophilic was evaluated. Core samples were sectioned into thin plates (5-7 mm thickness) using a diamond wafering saw. The rock surfaces were subsequently polished with P50 and P250 grit sandpaper to eliminate topological heterogeneity and ensure a consistent surface finish, followed by ultrasonic cleaning in distilled water. To induce a stable oleophilic wetting state, the prepared plates were aged in crude oil at 70 °C for 2 weeks. The wettability was quantitatively determined by measuring the static contact angle (θ) using a Drop Shape Analyzer (Krüss GmbH, Germany). A sessile drop of the aqueous phase (4 μL, distilled water) was deposited onto the rock surface. The contact angle was automatically calculated by the instrument's software using the Young-Laplace curve-fitting method to analyze the drop profile. A surface was classified as hydrophilic (water-wet) for $\theta < 90°$, hydrophobic (oil-wet) for $\theta > 90°$, and neutrally wet for $\theta \approx 90°$. The initial contact angle was measured for each oil-aged disc to establish a baseline wettability. Subsequently, the discs were immersed in the surfactant solutions at 70 °C. The temporal evolution of wettability alteration was monitored by measuring the contact angle at predetermined time intervals throughout the aging process.

2.5 Adsorption measurements

Static adsorption experiments were performed using carbonate rock powder (< 100 μm), prepared by Soxhlet extraction in chloroform followed by drying and mechanical crushing. Pure and encapsulated surfactant solutions at post-CMC concentrations were mixed with the rock powder at a 5 : 1 liquid/solid ratio. Sealed suspensions were aged at 70 °C for 24 h to achieve adsorption equilibrium, then centrifuged at 3,000 rpm for 30 min. The supernatant was subsequently filtered through 0.22 μm membrane filters to remove residual solids. The concentration of the surfactant in the filtrate was determined by Cary 6000 UV-Vis-NIR spectrophotometer (Agilent Technologies, USA) using calibration curves that were previously established for each surfactant system. Adsorption quantities were derived from initial-to-equilibrium concentration differentials normalized to rock mass.

2.6 Oil recovery factor

The displacement efficiency of pure and encapsulated surfactant formulations was assessed and compared using the spontaneous imbibition technique. Cylindrical rock cores were vacuum-saturated with crude oil by placing them in a high-pressure cell at 10 MPa for 24 h. The mass of each dry and saturated core was measured. The initial oil volume in place was calculated from the mass difference and the known density of the oil at the saturation temperature. The oil-saturated cores were then individually immersed in Amott cells containing 400 mL of the displacement fluid (i.e., brine, surfactant solution, or encapsulated surfactant solution). The cells were maintained at reservoir temperature (70 °C). Due to buoyancy forces arising from density differences, oil displaced from the core migrated upwards and accumulated in the graduated neck of the Amott cell. ORF was calculated as the ratio of the produced oil volume to the initial oil volume in the core pores, expressed as a percentage.

3. Results and discussion

3.1 Characterization

Surfactant nanocarriers were synthesized at 0.25% concentration for AEC and 0.12% for APG. The set concentrations were determined experimentally at which the solutions remain colloidally stable. The average carrier diameter was calculated from SEM images and zeta-potential. SEM images of the obtained carriers are demonstrated in Fig. 2.

For AEC, the average carrier size from SEM was 98.7 nm, from zeta-sizer was 117.7 nm. For APG, the lowest carrier size was 152.4 and 169.6 nm from SEM and zeta-sizer respectively. The lowest obtained size of APG-silica structures was 128.8 nm (Fig. 3). The obtained size of carriers satisfies the requirements for permeability of carbonate reservoirs, whose average pore size was determined as varying from hundreds of nanometers to millimeters (Xu et al., 2020).

To assess the chemical composition of obtained nanocarriers FTIR analysis was conducted. Fig. 4 presents the FTIR spectra of dried AEC- and APG-loaded silica nanocarriers. Both samples exhibit a pronounced peak at 1,108 cm^{-1}, which corresponds to the asymmetric stretching vibration of Si–O–Si, confirming the formation of the silica network. The band at 445 cm^{-1} is attributed to Si–O–Si bending modes, further supporting the successful condensation of the silica matrix during the sol-gel process. In addition to the silica framework vibrations, characteristic surfactant alkyl chain bands are clearly visible. The peaks at 2,922 and 2,852 cm^{-1} correspond to the asymmetric and symmetric CH_2 stretching vibrations of the hydrophobic carbon chains of AEC and APG. The asymmetric and symmetric CH_2 bands are more pronounced in AEC-loaded silica carriers compared to APG-loaded ones, suggesting a higher retention of the AEC within the silica matrix. This observation is consistent with the longer alkyl chain of AEC, which promotes stronger association with the silica during the sol-gel encapsulation process.

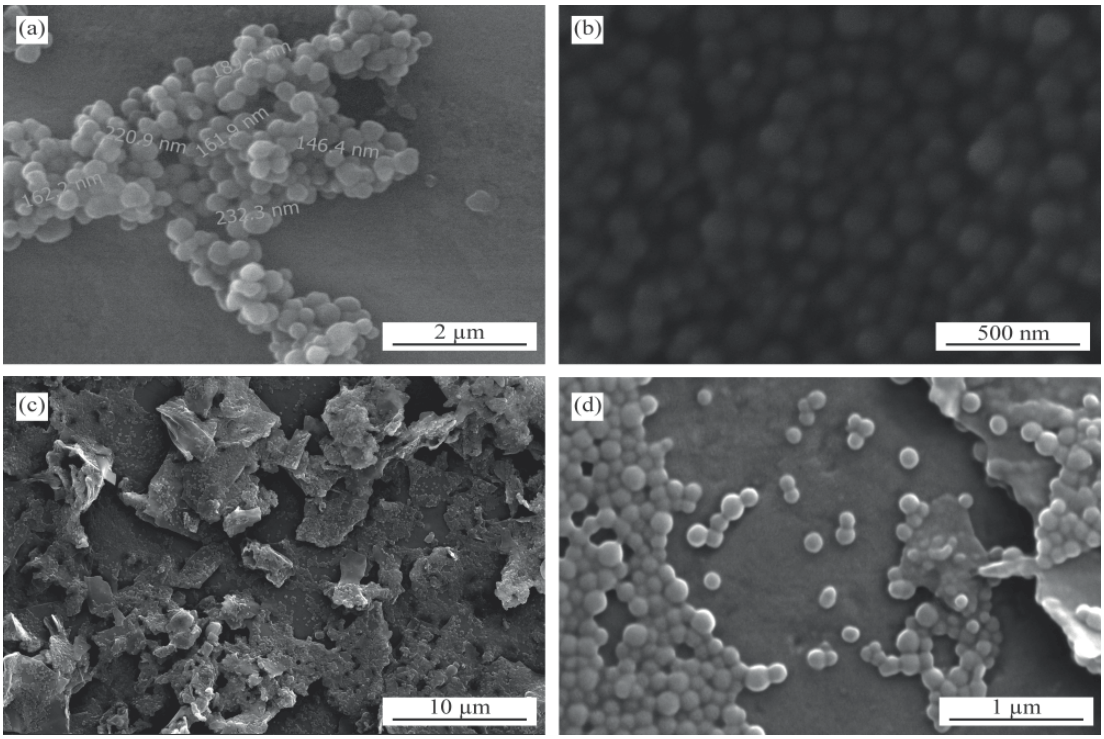

Fig. 2. SEM pictures of surfactant carriers: (a) APG, 2 µm, (b) APG, 500 nm, (c) AEC, 10 µm, and (d) AEC, 1 µm.

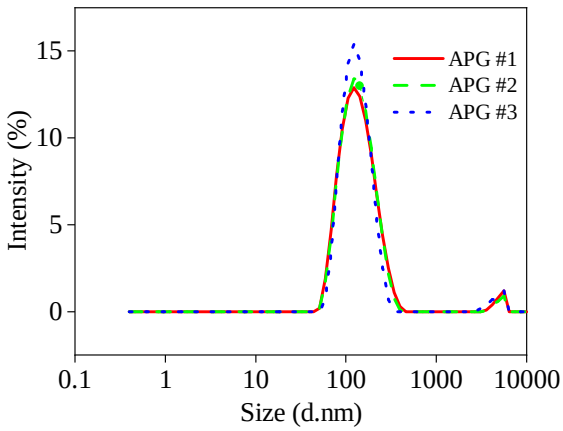

Fig. 3. APG size distribution by intensity (z. average = 128.4 d.nm).

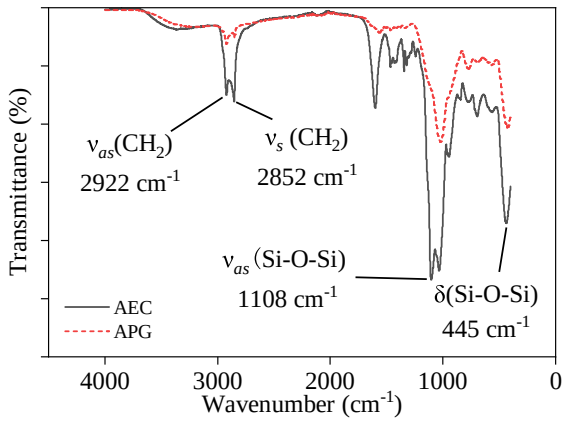

Fig. 4. FTIR spectra of silica nanocarriers.

3.2 IFT

3.2.1 IFT in distilled water

A fundamental property of surfactants is their capacity to reduce the IFT at the oil-water interface. Both experimental studies and field applications of surfactant flooding have established that IFT is a critical mechanism for achieving high displacement efficiency and enhancing oil recovery. Conventionally, one would anticipate the interfacial performance of an encapsulated surfactant, following its release, to be either diminished (in the case of incomplete release) or equivalent to that of its pure form. Contrary to this expectation, Cortés et al. (2018) reported a synergistic effect, where resin-based nanocapsules containing Span 20 and Petro 20 surfactants achieved a 99% greater reduction in IFT compared to the pure surfactants, underscoring the potential role of shell constituents in enhancing interfacial activity.

In this work, the carrier shell was composed of silica. The hypothesis is that upon triggered rupture, the released silica would persist in the bulk solution as SNPs and could potentially act in concert with the surfactant to improve interfacial performance. To evaluate this, the equilibrium IFT was measured for pure and encapsulated formulations of both surfactants after incubation at 70 °C. The investigated concentrations for AEC were 0.01, 0.05, 0.15, and 0.25 wt%, and for APG, 0.005, 0.01, 0.05, and 0.1 wt%. The stability threshold of the solution defined the upper concentration limit for each surfactant during the nanocarrier synthesis process.

For AEC, the IFT decreased sharply with increasing concentration up to 0.15wt%, beyond which the isotherm

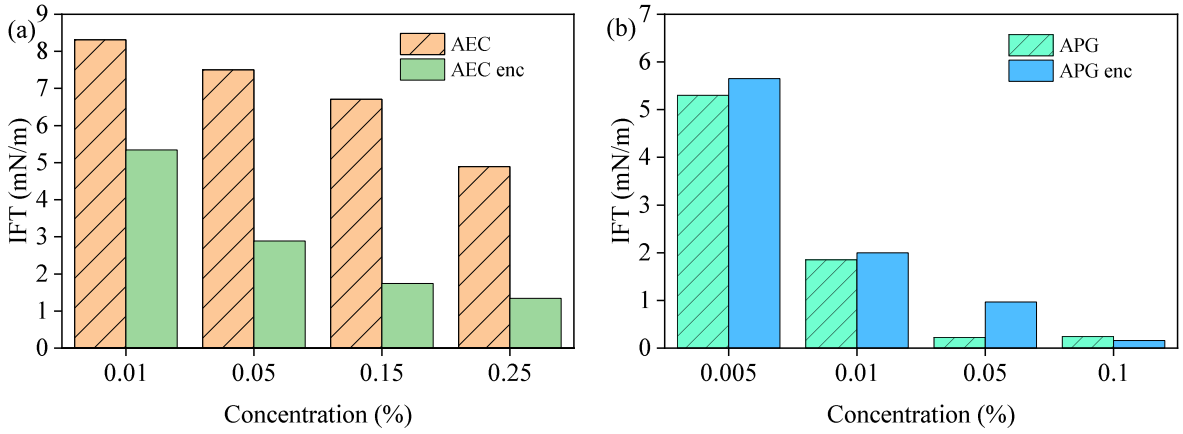

Fig. 5. IFT of (a) AEC and (b) APG in pure and encapsulated forms after heating under 70 °C.

plateaued (Fig. 5(a)). This behavior is indicative of interfacial saturation, where surfactant molecules fully occupy the available surface area. A synergistic effect between SNPs and surfactant was observed: On average, the encapsulated AEC solutions yielded IFT values that were 61.2% lower than those of pure counterparts at equivalent concentrations. The most significant disparity was recorded at 0.25 wt%, where the encapsulated system achieved an IFT of 1.34 mN/m, compared to 4.89 mN/m for the pure surfactant.

The attenuated difference in IFT at higher concentrations (>0.15 wt%) is consistent with an already surfactant-saturated interface. Under these conditions, any further reduction in IFT is likely governed by the co-adsorption and specific arrangement of SNPs at the interface, whose relative contribution becomes more significant as the surfactant's capacity to lower IFT alone is exhausted. For the nonionic surfactant APG, the IFT exhibited a characteristic dependence on concentration, as depicted in Fig. 5(b)). A sharp decrease in IFT was observed in the pre- and near-CMC regions (0.005-0.01 wt%), followed by a plateau at higher concentrations (0.05-0.1 wt%) as the interface became saturated and micellization commenced in the bulk solution.

In contrast to the anionic surfactant, the encapsulated APG formulation consistently showed a higher IFT across all concentrations, except at the maximum tested concentration (0.1 wt%). The most pronounced disparity was observed at 0.05 wt%, where the pure APG solution achieved an IFT of 0.22 mN/m, compared to 0.97 mN/m for its encapsulated counterpart.

Contrary to some literature suggesting nanoparticle presence has a negligible effect on IFT in the post-CMC region due to interfacial oversaturation (Jia et al., 2020), a significant concentration-dependent IFT reduction was observed for these systems even above the CMC. For instance, encapsulated AEC at 0.25 wt% achieved an IFT of 1.34 mN/m, notably lower than the 1.74 mN/m recorded at 0.15 wt%, indicating a continued role for SNPs beyond simple surfactant delivery. As these measurements were conducted in deionized water, the enhanced performance is unequivocally attributable to the presence of SNPs liberated from the carriers. This finding aligns with the work of Jia et al. (2020) who documented similar IFT reduction using hydrophilic SiO_2 nanoparticles. Most likely, electrostatic repulsion between the anionic headgroups of AEC and the negatively charged SNPs promotes better interfacial adsorption and a more densely packed surfactant film at the interface, thereby facilitating the observed additional IFT reduction (Ivanova et al., 2020). Besides, SNPs can carry the asphaltene molecules from the crude oil to oil-water interface, thereby additionally reducing IFT (Rezaei et al., 2022).

As for the APG, this diminished interfacial performance can be attributed primarily to the colloidal instability of the APG nanocarriers, which are more prone to aggregation, as demonstrated by the SEM images. This agglomeration is postulated to hinder the transport and accessibility of both surfactant molecules and SNPs to the oil-water interface. Furthermore, the interaction mechanism differs significantly from that of the anionic AEC system. In the absence of electrostatic forces for nonionic APG, the primary interactions with SNPs are hydrophobic attraction and hydrogen bonding. The silanol groups (Si – OH) on the SNP surface can form hydrogen bonds with the polyglucoside headgroup of APG. This can lead to the adsorption of surfactant molecules onto the nanoparticle aggregates, effectively sequestering them in the bulk phase and reducing the effective concentration available for interfacial activity. This phenomenon is similar to observations reported by Biswal and Singh (2016) for systems containing nanoparticles and the nonionic surfactant Tween 20.

The singular reduction in IFT for the encapsulated system at the highest concentration suggests a concentration-dependent shift in this equilibrium. It is hypothesized that at this elevated concentration, a sufficient number of surfactant molecules are present to saturate both the nanoparticle surfaces and the oil-water interface. Additionally, a carrier-effect, wherein surfactant-loaded SNPs co-adsorb at the interface, may contribute to the final IFT reduction, as discussed in other nanoparticle-surfactant systems (Zargartalebi et al., 2014).

3.2.2 Salinity effect on IFT

The influence of brine salinity, encompassing Na^+, Ca^{2+}, and Mg^{2+} ions, on the IFT of both pure and encapsulated

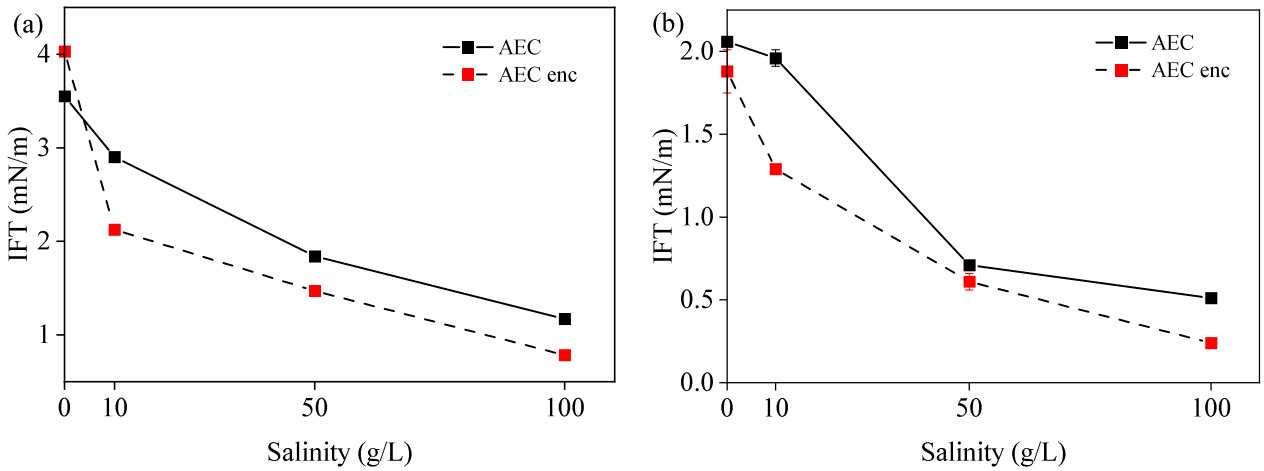

Fig. 6. IFT of pure and encapsulated AEC (0.1%) on the interface with oil at (a) 25 °C and (b) 70 °C at different water salinities.

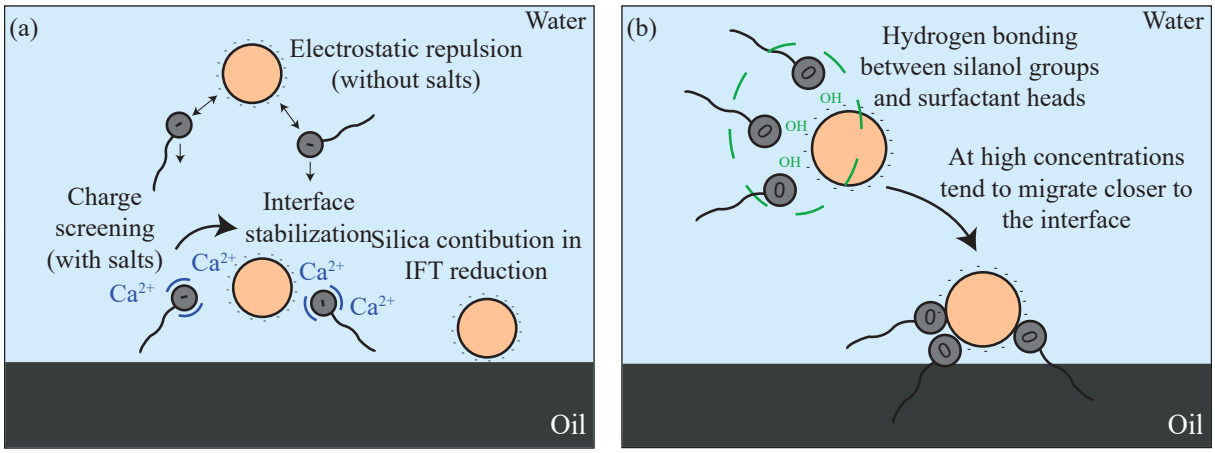

Fig. 7. Interaction mechanisms of encapsulated (a) AEC and (b) APG with oil in presence of SNPs (orange) after surfactant release.

surfactant formulations was systematically evaluated at 25 and 70 °C. Under these conditions, the encapsulated AEC consistently outperformed its pure counterpart (e.g., 2.13 vs. 2.9 mN/m at 10 g/L salinity) (Fig. 6), a phenomenon attributed to two synergistic factors: Salt-induced acceleration of surfactant release from the carriers and cation-mediated screening that fosters favorable interactions between the surfactant and the co-released SNPs, consistent with findings by Alsmaeil et al. (2021).

The key mechanisms governing the interaction between surfactants and SNPs vary with surfactant type: For the anionic AEC electrostatic interactions play the dominant role, whereas for the nonionic APG hydrogen bonding and Van der Waals forces primarily drive the association (Fig. 7).

In contrast, the nonionic APG system displayed markedly different behavior (Fig. 8). The IFT of pure APG solutions exhibited a minor yet consistent increase upon salt addition, irrespective of concentration, with values stabilizing at 0.317 ± 0.013 mN/m (25 °C) and 0.616 ± 0.046 mN/m (70 °C) across a 10-100 g/L salinity range. For encapsulated APG, elevated temperature and salinity triggered carrier rupture and release, leading to a reduction in IFT reduction from the initial aggregated state.

The aggregated data of salinity effect on IFT of pure and encapsulating surfactants is compiled in Table 1. For the anionic AEC surfactant, the introduction of electrolytes (1 wt%) reduced the IFT for both pure and encapsulated forms. This salting-out effect compresses the electrical double layer and mitigates electrostatic repulsion between anionic headgroups, thereby promoting a denser molecular packing at the oil-water interface (Liu et al., 2013; Scerbacova et al., 2023). Divalent ions can bind to surfactant head groups, increasing the coverage ratio at the interface and thereby lowering IFT (Liu et al., 2013). The effect is particularly pronounced for divalent cations (Ca^{2+}, Mg^{2+}), which can act as bridging agents between surfactant molecules, further enhancing interfacial cohesion and reducing IFT, as supported by molecular dynamics simulations (Yan et al., 2011).

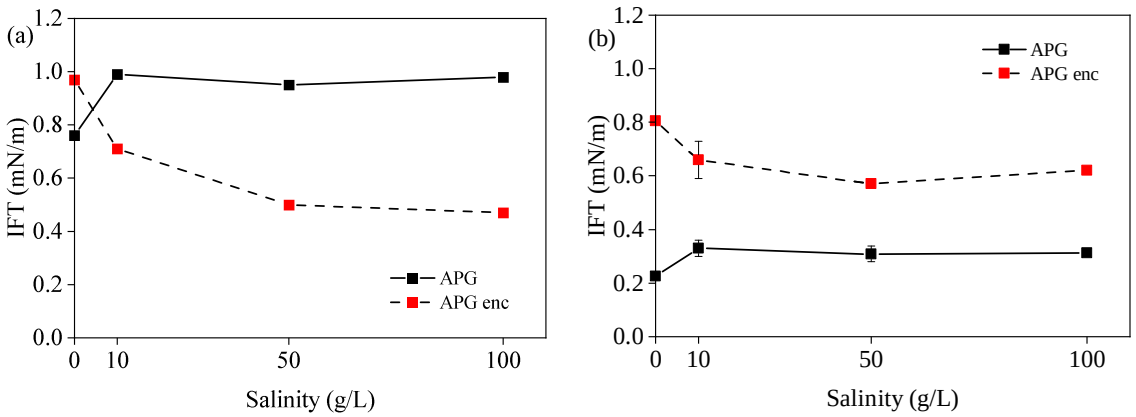

Fig. 8. IFT of pure and encapsulated APG (0.05%) on the interface with oil at (a) 25 °C and (b) 70 °C at different water salinities.

Table 1. IFT values of pure and encapsulated (enc.) AEC and APG solutions at various salinity level and temperatures.

Surfactant	Salinity (g/L)	IFT (mN/m)			
		Pure (25 °C)	Enc. (25 °C)	Pure (70 °C)	Enc. (70 °C)
AEC	0	3.55	4.03	2.06	1.88
	10	2.90	2.13	1.96	1.29
	50	1.84	1.47	0.71	0.61
	100	1.17	1.78	0.51	0.24
APG	0	0.76	0.97	0.23	0.81
	10	0.99	0.71	0.33	0.66
	50	0.95	0.5	0.31	0.57
	100	0.98	0.47	0.31	0.62

However, at 70 °C in saline environments, the IFT of the encapsulated formulation remained significantly higher than that of the pure surfactant. This is rationalized by a loss of colloidal stability under these conditions, leading to silica sedimentation, as shown in Fig. S1 in the Supplementary file. Interestingly, it occurs only under both elevated temperature and salinity. A substantial fraction of the released nonionic surfactant molecules adsorb onto the surfaces of the aggregating SNPs via hydrogen bonding and hydrophobic interactions (Bharti et al., 2012; Pichot et al., 2012).

3.3 Wettability

Rock wettability is a fundamental property governing fluid distribution and displacement dynamics within porous media. Carbonate reservoirs are typically characterized by an initial oil-wet or mixed-wet state, a condition that promotes the preferential flow of water through larger pore channels and significantly constrains the efficiency of aqueous flooding processes (Anderson, 1987; Deng et al., 2020).

To simulate reservoir conditions, core samples were aged in crude oil for two weeks. The mean initial contact angles after aging were 91.1° for the AEC series and 95.1° for the APG series. These samples were subsequently put to surfactant solutions at 70 °C across a range of salinities.

The efficacy of both pure and encapsulated formulations in altering wettability is quantified in Fig. 9. For the anionic AEC surfactant, wettability alteration was strongly dependent on ionic strength. In deionized water, the pure AEC solution reduced the contact angle from 89° to 64° ± 4° after 24 h, with a further decrease to 62° ± 2° observed after 7 days. In contrast, a pronounced enhancement in performance was observed in high-salinity brine (100 g/L total dissolved solids), where the contact angle decreased from 93° to 49° ± 3° over the same period. This significant improvement in hydrophilicity under saline conditions is consistent with the IFT trends earlier-reported and can be attributed to more favorable surfactant packing and interactions at the solid-liquid interface facilitated by electrolyte screening and divalent cation bridging effects.

The encapsulated AEC formulation exhibited a marginally lower contact angle compared to its pure counterpart in deionized water. A pronounced enhancement in wettability alteration was observed at elevated salinity (100 g/L). Under these conditions, the release of the surfactant from the nanocarriers was significantly accelerated, culminating in a substantial reduction in the contact angle from 98° to 37° ± 8° over a seven-day aging period. A similar trend was observed for the APG surfactant, where an increase in salinity generally led to a systematic decrease in the contact angle for both the pure and encapsulated forms. Notably, the encapsulated APG consistently yielded statistically significantly lower contact angles than the pure surfactant after both 1 and 7 days of exposure to the brine solution.

The full set of wettability data is summarized in Table 2. Increasing salinity also enhanced the wettability alteration efficiency of APG, with the improvement being particularly pronounced for the encapsulated formulation. In deionized water, encapsulated APG reduced the contact angle to 30.1° ± 3.0° after 7 days, while the addition of 10 g/L salinity further lowered it to 21.8° ± 2.0°. The strongest effect was observed at

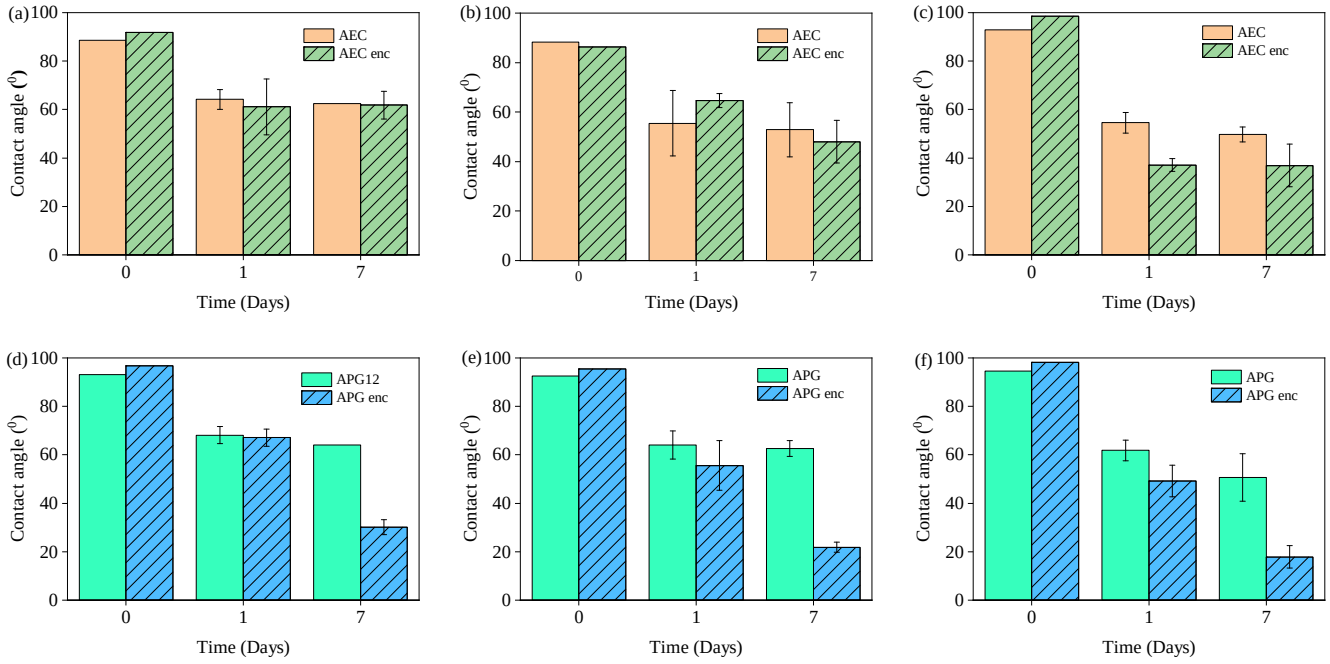

Fig. 9. Contact angle between water drop on carbonate rock surface before (0 days) and after (1 and 7 days) aging in surfactant at varying salinity: (a) AEC, salinity: 0 g/L, (b) AEC, 10 g/L, (c) AEC, 100 g/L, (d) APG, 0 g/L, (e) APG, 10 g/L, and (f) APG, 100 g/L.

Table 2. Contact angle evolution under different salinity conditions after aging in pure and encapsulated (enc.) surfactant solutions.

Surfactant	Salinity (g/L)	Contact angles (°)					
		0 day		1 day		7 days	
		Pure	Enc.	Pure	Enc.	Pure	Enc.
AEC	0	88.5	91.9	64.2 ± 4	61.0 ± 9.9	62.5	61.8 ± 5.7
	10	88.2	86.3	55.5 ± 9.9	64.7 ± 2.8	52.9 ± 9.8	48.0 ± 8.6
	100	93.0	98.6	54.6 ± 4.3	37.1 ± 2.6	49.8 ± 3.0	36.9 ± 8.8
APG	0	93.1	96.8	68.1 ± 3.5	67.1 ± 3.6	64.1	30.1 ± 3.1
	10	92.5	95.5	64.1 ± 5.8	55.6 ± 9.9	62.6 ± 3.3	21.8 ± 2.1
	100	94.5	98.1	61.9 ± 4.2	49.2 ± 6.6	50.7 ± 9.8	17.9 ± 4.7

100 g/L salinity, where the encapsulated APG system achieved a minimum contact angle of 18° ± 5° after 7 days, indicating a transition to a strongly water-wet regime (Fig. 10).

These results clearly demonstrate that encapsulation consistently improves the wettability shift toward more water-wet conditions, particularly under high salinity, indicating a stronger overall displacement potential for carbonate reservoirs. Wettability alteration resulting from the application of pure and encapsulated surfactant formulations proceeds via two distinct mechanisms: Surfactant-rock interfacial interactions and nanoparticle-induced interactions. The primary mechanisms for surfactant-induced wettability alteration are categorized as coating and cleaning (Hammond and Unsal, 2010, 2011). The coating mechanism occurs through hydrophobic interactions between the surfactant tail and the oil layer of adsorbed carboxylic groups on the rock surface. The cleaning mechanism involves washing away desorbed oil from the rock. It is generally accepted that anionic surfactants cannot permanently desorb oil components from the rock surface via the direct cleaning mechanism (Standnes and Austad, 2000). Instead, these surfactants typically form a bilayer structure at the rock-fluid interface. In this configuration, the surfactant head groups extend into the aqueous phase, establishing a hydrophilic layer that promotes oil displacement. This bilayer mechanism has also been demonstrated for nonionic surfactants (Das et al., 2018).

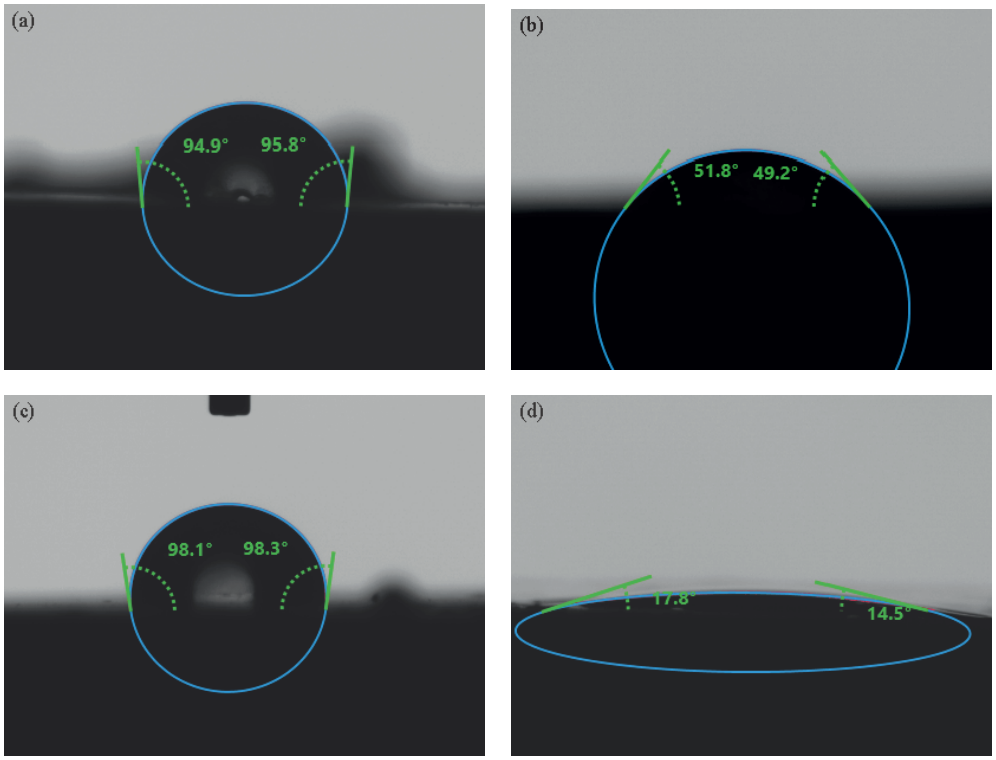

Fig. 10. Pictures of DW drops on carbonate rock surface: (a) Before aging in pure APG, (b) after 7 days aging in pure APG, (c) before aging in encapsulated APG, and (d) after 7 days aging in encapsulated APG.

The superior performance observed for encapsulated systems cannot be explained by surfactant release alone. The effect of interfacial activity of SNPs has been repeatedly mentioned in the literature (Kesarwani et al., 2021; Du et al., 2026). SNPs co-released during carrier rupture actively contribute to wetting transition through two cooperative mechanisms: Surface charge alteration and generation of structural disjoining pressure.

First, SNPs alone can modify wettability by altering surface charge. Hydration of SNPs generates negatively charged SiO^- surface sites enabling them to compete with naturally occurring anionic carboxylates for adsorption sites on the positively charged carbonate surface. Successful adsorption shifts the surface wettability toward water-wet conditions. This process is highly condition-dependent, with efficacy governed by solution chemistry. Notably, the presence of divalent cations (e.g., Ca^{2+}) significantly enhances SNP adsorption onto carbonates by mitigating electrostatic repulsion and potentially acting as ionic bridges, thereby facilitating the displacement of organic material (Alzobaidi et al., 2021).

Another contributing mechanism is the generation of structural disjoining pressure. SNPs can penetrate the thin aqueous film between the rock surface and adhered oil phase, forming a structured nanoparticle wedge (Li et al., 2017). The resulting entropic and osmotic forces generate a repulsive pressure that overcomes the adhesion energy, destabilizing and ultimately detaching the oil droplet.

3.4 Static adsorption

Surfactant adsorption mitigation is the key objective of encapsulation; therefore, demonstrating that these nanocompositions are able to reduce surfactant retention is essential for evaluating both the technical and economic feasibility of the proposed EOR concept. Conceptually, the use of nanocarriers offers a dual protective action: During transport through the porous medium and within the target treatment zone. Static adsorption experiments were performed to evaluate surfactant loss during equilibration with crushed carbonate rock at reservoir-representative salinity conditions. Fig. 11(a) displays the adsorption behavior of AEC surfactant, while Fig. 11(b) summarizes the adsorption data obtained for APG.

The adsorption of the neat AEC increased from approximately 2.15 mg/(g of rock) at 0.10 wt% to 4.87 mg/(g of rock) at 0.25 wt%. When encapsulated, the AEC adsorption values were significantly reduced, by about 45%-47% at all tested concentrations. In contrast, APG exhibited considerably lower adsorption magnitudes in the same salinity conditions. The adsorption of neat APG varied only between 0.45 and 0.69 mg/(g of rock) within 0.05-0.10 wt%. Encapsulation resulted in only minor changes (1%-13%), reflecting the weak inherent interaction between APG and the carbonate surface.

The adsorption of ionic surfactants such as AEC on calcite is mainly driven by strong electrostatic interactions between the negatively charged carboxylate headgroup and oppositely charged rock surface. This mechanism leads to relatively high retention levels consistent with previously reported adsorption

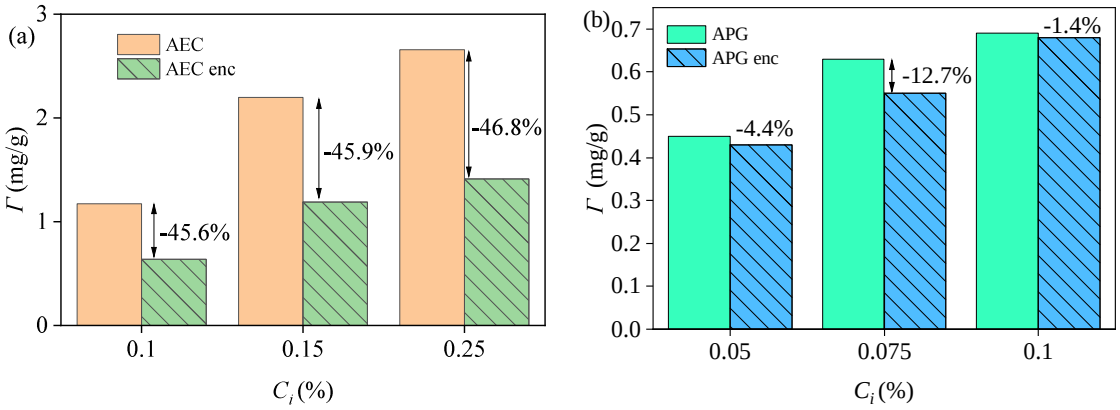

Fig. 11. Static adsorption of pure and encapsulated (a) AEC and (b) APG.

magnitudes for ethoxylated carboxylates on carbonates (Scerbacova et al., 2023).

In contrast, APG exhibits inherently weak affinity toward calcite due to the absence of ionic binding sites in its molecular structure. Its adsorption is primarily governed by van der Waals interactions and hydrogen bonding of the glucose units, and therefore remains low even above the CMC (Suh et al., 2017). Nevertheless, the encapsulated APG formulations displayed a slight reduction in adsorption, which agrees with prior observations for nonionic glucosides.

Overall, both systems demonstrated adsorption suppression upon encapsulation, confirming the effectiveness of this strategy for minimizing chemical losses in carbonate formations A plausible mechanism involves the presence of residual silica fragments originating from silica carrier degradation, which can occupy reactive sites on the mineral surface and reduce the available adsorption area. As a result, fewer surfactant molecules are able to adsorb directly onto calcite. Similar nanoparticle-assisted shielding effects have been widely documented for both ionic and nonionic surfactants (Liu et al., 2021b; Scerbacova et al., 2022). Moreover, the less pronounced mitigation for APG may arise from preferential adsorption of APG onto silica surfaces, consistent with the behavior discussed in Section 3.2.2 (Salinity effect on IFT) and recent studies demonstrating APG-silica affinity (Zhong et al., 2019).

From an EOR perspective, the substantial reduction in adsorption achieved for AEC indicates a more efficient delivery of the active chemical to the pore network, enabling improved interfacial performance and reduced chemical expenditure.

3.5 Oil recovery factor

Prior to conducting spontaneous imbibition experiments, the wettability of the carbonate rock cores was quantified to ensure appropriate initial conditions by contact angle measurements. Freshly cleaned samples exhibited a water-wet contact angle of 72°, while 2-week aging in crude oil at 70 °C increased the contact angle to $97° \pm 3°$. This oil-wet starting condition provides a relevant baseline for evaluating the extent to which the tested systems are able to restore water-wetness and thereby initiate capillary-driven oil displacement.

The efficacy of high salinity water (HSW), along with pure and encapsulated surfactant formulations, in enhancing oil recovery is shown in Fig. 12. The ORF was quantified as the volume of oil displaced via spontaneous imbibition in an Amott cell. For the anionic surfactant (AEC), the pure surfactant solution showed superior oil displacement efficiency compared to its encapsulated counterpart during the first 4 h of the imbibition test. However, after 8 h, the encapsulated AEC solution achieved an ORF of 15.9%, surpassing the pure solution (14.5%) and HSW (7.9%). Beyond this time, the encapsulated system consistently outperformed the pure surfactant, ultimately yielding a final ORF approximately 10% higher at the conclusion of the 168-hour test, after which all systems reached a recovery plateau.

A more pronounced delayed-release effect was observed for the APG surfactant. The pure APG solution maintained a higher recovery factor than the encapsulated form for the first 48 h. A subsequent sharp increase in the recovery rate for the encapsulated APG coincided with the hypothesized release of the surfactant cargo. At the plateau stage, the cumulative ORF for the encapsulated APG system was 3% greater than that of the pure surfactant. Most likely, start of the plateau stage is associated with maximum achievable interfacial modification: Both the oil-water IFT and rock wettability reach near-steady values.

The zoom-in view reveals that even during the earliest stage of imbibition, a measurable increase in ORF accompanies the initial release of surfactant into the aqueous phase. This effect is attributed to the rapid onset of IFT reduction, which requires only a small fraction of the total surfactant payload to reach the oil-water interface, thereby immediately enhancing capillary-driven displacement.

This enhanced performance is also attributed to a proposed mechanism wherein, following surfactant release, SNPs compete with surfactant molecules for adsorption sites on the rock surface. This competition reduces surfactant loss to the rock matrix, thereby maintaining a higher surfactant concentration in the aqueous phase. This effect contributes to lower IFT and, consequently, a higher ultimate ORF in the encapsulated

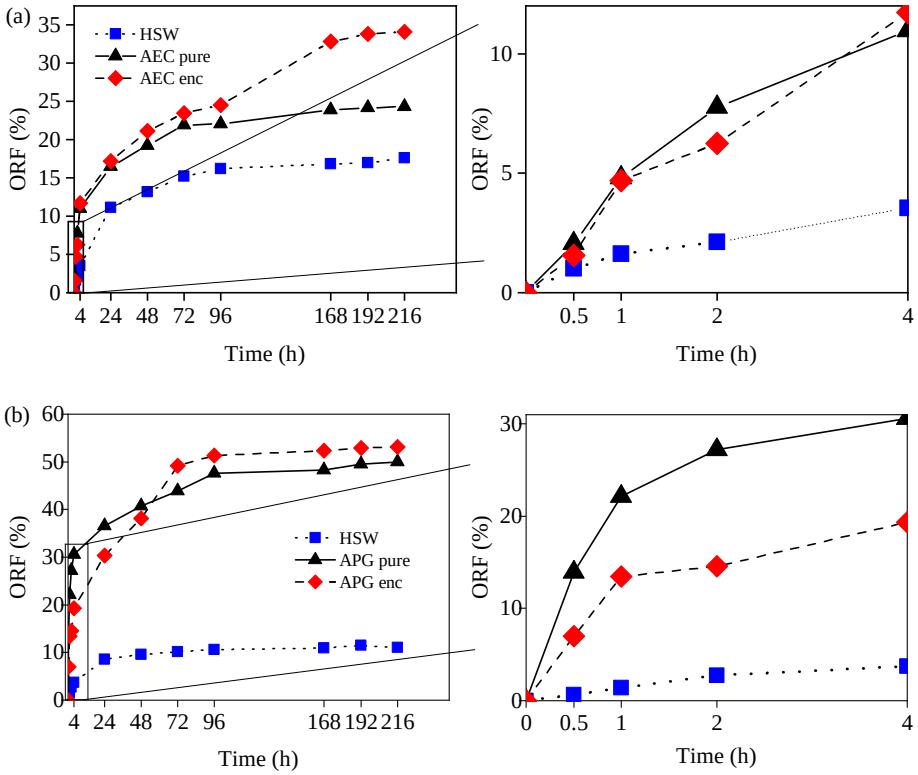

Fig. 12. Oil recovery factor by time from spontaneous imbibition tests with HSW, pure, encapsulated (a) AEC and (b) APG surfactants.

systems.

Both IFT reduction, wettability alteration and surfactant adsorption mitigation strongly contribute to the improvement of ORF. All mechanisms driving ORF enhancement are consolidated and schematically illustrated in Fig. 13. It is critical to note that surfactant interfacial behavior and adsorption kinetics are highly dependent on flow dynamics. This was highlighted in the core-flooding study by Alhassawi and Romero-Zerón (2015b) utilizing sodium dodecyl sulfate encapsulated in β-cyclodextrin. Their results indicated only a marginal improvement in oil recovery during the injection of the encapsulated surfactant slug. However, a subsequent water flood was significantly more effective with the encapsulated surfactant than with the pure surfactant, suggesting a controlled-release mechanism that mitigates adsorption and improves sweep efficiency during post-flush. This underscores the limitation of static imbibition tests and emphasizes the need to evaluate surfactant performance under dynamic core-flooding conditions to assess its potential for EOR applications accurately.

From a field-scale perspective, the performance of the developed AEC and APG nanocarriers primary indicates their suitability for carbonate reservoir conditions. The sub-150 nm carrier size supports deep propagation through carbonate pore-throat networks without pore blocking, while high salinity and elevated temperatures ensure gradual controlled release of the active surfactant within the target zone. The tested surfactant concentrations (0.05-0.25 wt%) fall well within the lower end of typical field-scale EOR surfactant slugs. Moreover, the enhanced interfacial performance (IFT reduction and wettability alteration) observed for the encapsulated formulations implies that comparable or even improved displacement efficiencies may be achievable at lower chemical dosages, offering a substantial economic advantage for field-scale implementation.

4. Conclusions

This study demonstrates that encapsulating anionic (AEC) and nonionic (APG) surfactants within SNPs significantly enhances their performance in reducing IFT, altering wettability, mitigating adsorption and improving oil recovery under simulated carbonate reservoir conditions ultimately.

The thermally triggered rupture of the nanocarriers facilitated a sustained release of the surfactant cargo. For the anionic AEC, encapsulation resulted in markedly lower IFT values compared to its pure form. This is attributed to electrostatic repulsion between the negatively charged SNPs and the anionic surfactant headgroups, which effectively limited surfactant adsorption onto the positively charged carbonate rock and promoted a higher concentration of active molecules at the oil-water interface. While high salinity (100 g/L) induced ion screening and attenuated this electrostatic effect, the interfacial stabilization provided by the SNPs still ensured superior IFT performance.

Encapsulated systems achieved a more profound and rapid shift toward water-wet conditions than pure surfactants over a 7-day aging period. The most significant alteration was

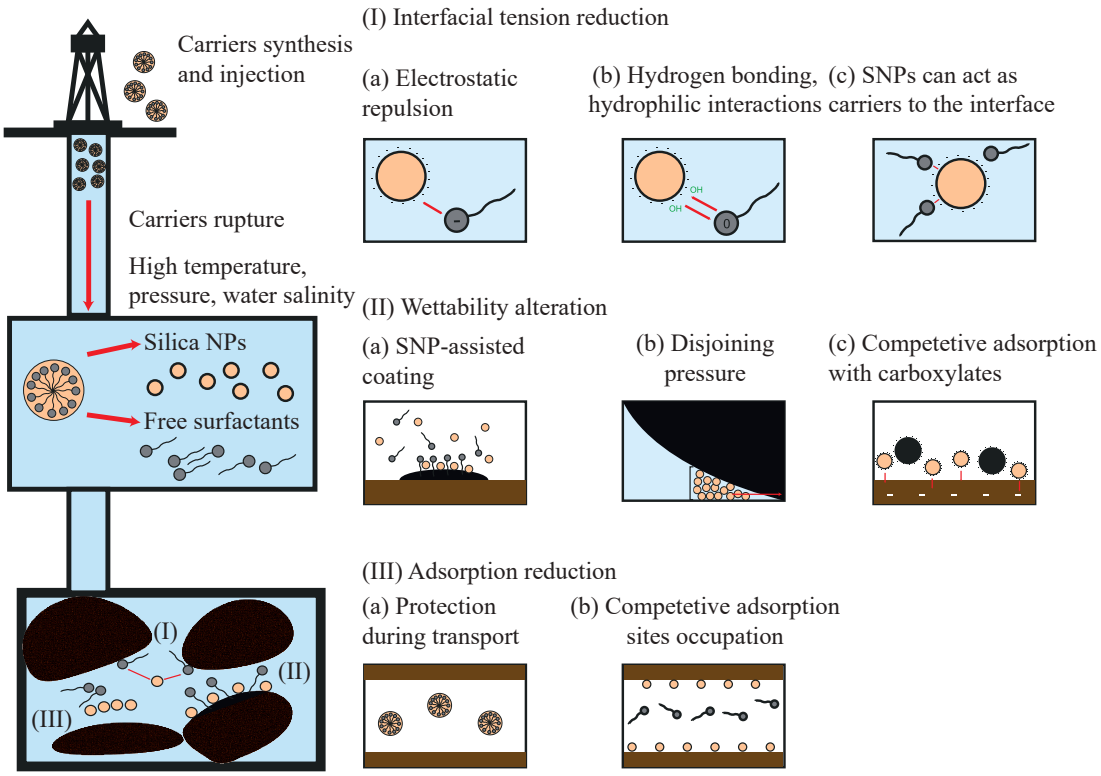

Fig. 13. Conceptual mechanistic pathway of silica nanocarriers for EOR in carbonate reservoirs.

observed for encapsulated APG at high salinity, reducing the contact angle to $18^\circ \pm 5^\circ$. This enhancement is mechanistically linked to three synergistic effects: (i) SNP-assisted coating of the rock surface, (ii) the generation of structural disjoining pressure by nanoparticles, and (iii) competitive adsorption of SNPs onto carbonate sites, displacing oil components.

Spontaneous imbibition tests quantitatively confirmed the technological advantage of encapsulation, yielding a 10% increase in the ultimate ORF for AEC and a 3% increase for APG over their pure surfactant counterparts. The delayed release kinetics, adsorption reduction and enhanced interfacial properties of the encapsulated surfactants proved advantageous for sustained mobilization of oil.

In summary, the performance enhancement stems from the synergistic interplay between the released surfactants and the carrier SNPs, mediated by a combination of electrostatic, hydrophobic, and hydrogen-bonding interactions. These results affirm the potential of surfactant encapsulation as an effective strategy for improving EOR in challenging carbonate formations.

Future work should focus on dynamic core-flooding experiments and long-term stability assessments to fully evaluate the field applicability of this technology under realistic reservoir conditions.

Acknowledgements

The authors express their gratitude to the Laboratory of Low-Temperature Chemistry, Department of Chemistry, Lomonosov Moscow State University, for their assistance in the characterization of the nanocarriers.

Additional information: Author's email

megycd@163.com (C. Yuan).

Supplementary file

https://doi.org/10.46690/ager.2025.12.06

Conflict of interest

The authors declare no competing interest.

References

Ahsaei, Z., Parsaei, R., Kalantariasl, A., et al. Slow release of surfactant by smart thermosensitive polymer-functionalized mesoporous silica for enhanced oil recovery: Synthesis and characterization. Journal of Molecular Liquids, 2024, 414: 126216.

Ahsaei, Z., Parsaei, R., Kalantariasl, A., et al. Enhanced oil recovery through controlled surfactant release from thermosensitive polymer-functionalized mesoporous silica: Interfacial tension, wettability, surfactant adsorption, and emulsification performance. Colloids and Surfaces A: Physicochemical and Engineering Aspects, 2025, 725: 137550.

Alhassawi, H., Romero-Zerón, L. New surfactant delivery system for controlling surfactant adsorption onto solid surfaces. Part I: Static adsorption tests. Canadian Journal

of Chemical Engineering, 2015a, 93(6): 1111-1120.

Alhassawi, H., Romero-Zerón, L. Novel surfactant delivery system for controlling surfactant adsorption onto solid surfaces. Part II: Dynamic adsorption tests. Canadian Journal of Chemical Engineering, 2015b, 93(8): 1371-1379.

Alhassawi, H., Romero-Zerón, L. Novel surfactant delivery system for controlling surfactant adsorption onto solid surfaces. Part III: Oil displacement tests. Canadian Journal of Chemical Engineering, 2015c, 93(8): 1539-1546.

Alsmaeil, A. W., Hammami, M. A., Enotiadis, A., et al. Encapsulation of an anionic surfactant into hollow spherical nanosized capsules: Size control, slow release, and potential use for enhanced oil recovery applications and environmental remediation. ACS Omega, 2021, 6(6): 3924-3933.

Alvarez Jürgenson, G., Bittner, C., Kurkal-Siebert, V., et al. Alkyl ether carboxylate surfactants for chemically enhanced oil recovery in harsh field conditions. Paper SPE 174589 Presented at SPE Asia Pacific Enhanced Oil Recovery Conference, Kuala Lumpur, Malaysia, 11-13 August, 2015.

Alzobaidi, S., Wu, P., Da, C., et al. Effect of surface chemistry of silica nanoparticles on contact angle of oil on calcite surfaces in concentrated brine with divalent ions. Journal of Colloid and Interface Science, 2021, 581: 656-668.

Anderson, W. G. Wettability literature survey Part 5: The effects of wettability on relative permeability. Journal of Petroleum Technology, 1987, 39: 1453-1468.

Belhaj, A. F., Aris B. M. Shuhli, J., Elraies, K. A., et al. Partitioning behaviour of novel surfactant mixture for high reservoir temperature and high salinity conditions. Energy, 2020a, 198: 117319.

Belhaj, A. F., Elraies, K. A., Mahmood, S. M., et al. The effect of surfactant concentration, salinity, temperature, and pH on surfactant adsorption for chemical enhanced oil recovery: A review. Journal of Petroleum Exploration and Production Technology, 2020b, 10: 125-137.

Bharti, B., Meissner, J., Gasser, U., et al. Surfactant adsorption and aggregate structure at silica nanoparticles: Effects of particle size and surface modification. Soft Matter, 2012, 8(24): 6573-6580.

Biswal, N. R., Singh, J. K. Interfacial behavior of nonionic Tween 20 surfactant at oil-water interfaces in the presence of different types of nanoparticles. RSC Advances, 2016, 6(114): 113307-113314.

Chang, Z., Chen, X., Peng, Y. The adsorption behavior of surfactants on mineral surfaces in the presence of electrolytes: A critical review. Minerals Engineering, 2018, 121: 66-76.

Cortés, F. B., Lozano, M., Santamaria, O., et al. Development and evaluation of surfactant nanocapsules for chemical enhanced oil recovery (EOR) applications. Molecules, 2018, 23(7): 1523.

Das, S., Nguyen, Q., Patil, P. D., et al. Wettability alteration of calcite by nonionic surfactants. Langmuir, 2018, 34(37): 10650-10658.

Deng, X., Kamal, M. S., Patil, S., et al. A review on wettability alteration in carbonate rocks: Wettability modifiers. Energy & Fuels, 2020, 34: 31-54.

Du, D., Hou, S., Pu, W., et al. Investigation on enhanced oil recovery potential of active nano-SiO_2 in high-temperature and high-salinity reservoirs at core and pore scale. Fuel, 2026, 404: 136363.

Falcone, J. S., Krumrine, P. H., Schweiker, G. C. The use of inorganic sacrificial agents in combination with surfactants in enhanced oil recovery. Journal of the American Oil Chemists' Society, 1982, 59(10): 369-375.

Hammond, P. S., Unsal, E. Forced and spontaneous imbibition of surfactant solution into an oil-wet capillary: The effects of surfactant diffusion ahead of the advancing meniscus. Langmuir, 2010, 26(9): 6206-6221.

Hammond, P. S., Unsal, E. Spontaneous imbibition of surfactant solution into an oil-wet capillary: Wettability restoration by surfactant-contaminant complexation. Langmuir, 2011, 27(8): 4412-4429.

Ivanova, A. A., Phan, C., Barifcani, A., et al. Effect of nanoparticles on viscosity and interfacial tension of aqueous surfactant solutions at high salinity and high temperature. Journal of Surfactants and Detergents, 2020, 23(2): 327-338.

Ivanova, A. A., Kozyreva, Z. V., Chekalov, A. Y., et al. Development and characterization of nanostructured surfactant compositions with prolonged action and stimuli-responsive physicochemical properties. Colloids and Surfaces A: Physicochemical and Engineering Aspects, 2024, 687: 133396.

Jia, H., Huang, W., Han, Y., et al. Systematic investigation on the interaction between SiO_2 nanoparticles with different surface affinity and various surfactants. Journal of Molecular Liquids, 2020, 304: 112777.

Kesarwani, H., Sharma, S., Mandal, A. Application of novel colloidal silica nanoparticles in the reduction of adsorption of surfactant and improvement of oil recovery using surfactant-polymer flooding. ACS Omega, 2021, 6(17): 11327-11339.

Li, R., Jiang, P., Gao, C., et al. Experimental investigation of silica-based nanofluid enhanced oil recovery: The effect of wettability alteration. Energy & Fuels, 2017, 31: 188-197.

Liu, Z., Hedayati, P., Ghatkesar, M. K., et al. Reducing anionic surfactant adsorption using polyacrylate as sacrificial agent investigated by QCM-D. Journal of Colloid and Interface Science, 2021a, 585: 1-11.

Liu, Z., Zhang, L., Cao, X., et al. Effect of electrolytes on interfacial tensions of alkyl ether carboxylate solutions. Energy & Fuels, 2013, 27: 3122-3129.

Liu, Z., Zhao, G., Brewer, M., et al. Comprehensive review on surfactant adsorption on mineral surfaces in chemical enhanced oil recovery. Advances in Colloid and Interface Science, 2021b, 294: 102467.

Lv, W., Zhou, Z., Zhang, Q., et al. Study on the mechanism of surfactant flooding: Effect of betaine structure. Advances in Geo-Energy Research, 2023, 10(3): 146-158.

Mushtaq, M., Tan, I. M., Rashid, U., et al. Effect of pH on the static adsorption of foaming surfactants on Malaysian

sandstone. Arabian Journal of Geosciences, 2015, 8(10): 8539-8548.

Ojo, O. F., Farinmade, A., John, V., et al. A nanocomposite of halloysite/surfactant/wax to inhibit surfactant adsorption onto reservoir rock surfaces for improved oil recovery. Energy & Fuels, 2020, 34(7): 8074-8084.

Olajire, A. A. Review of ASP EOR (alkaline-surfactant-polymer enhanced oil recovery) technology in the petroleum industry: Prospects and challenges. Energy, 2014, 77: 963-982.

Pichot, R., Spyropoulos, F., Norton, I. T. Competitive adsorption of surfactants and hydrophilic silica particles at the oil-water interface: Interfacial tension and contact angle studies. Journal of Colloid and Interface Science, 2012, 377: 396-405.

Rezaei, A., Khodabakhshi, A., Esmaeili, A., et al. Effects of initial wettability and different surfactant-silica nanoparticles flooding scenarios on oil recovery from carbonate rocks. Petroleum, 2022, 8(4): 499-508.

Rosestolato, J. C. S., Pérez-Gramatges, A., Lachter, E. R., et al. Lipid nanostructures as surfactant carriers for enhanced oil recovery. Fuel, 2019, 239: 403-412.

Saha, R., Uppaluri, R. V. S., Tiwari, P. Effect of mineralogy on the adsorption characteristics of surfactant-reservoir rock system. Colloids and Surfaces A: Physicochemical and Engineering Aspects, 2017, 531: 121-132.

Scerbacova, A., Ivanova, A., Grishin, P., et al. Application of alkalis, polyelectrolytes, and nanoparticles for reducing adsorption loss of novel anionic surfactant in carbonate rocks at high salinity and temperature conditions. Colloids and Surfaces A: Physicochemical and Engineering Aspects, 2022, 653: 129996.

Scerbacova, A., Kozlova, E., Barifcani, A., et al. Rock-fluid interactions of alkyl ether carboxylate surfactants with carbonates: Wettability alteration, ζ-potential, and adsorption. Energy & Fuels, 2023, 37(5): 3723-3740.

ShamsiJazeyi, H., Hirasaki, G. J., Verduzco, R. Sacrificial agent for reducing adsorption of anionic surfactants. Paper SPE 164061 Presented at SPE International Conference on Oilfield Chemistry, The Woodlands, Texas, USA, 8-10 April, 2013.

Sharma, H., Dufour, S., Arachchilage, G. W. P. P., et al. Alternative alkalis for ASP flooding in anhydrite containing oil reservoirs. Fuel, 2015, 140: 407-420.

Standnes, D. C., Austad, T. Wettability alteration in chalk. Journal of Petroleum Science and Engineering, 2000, 28(3): 123-143.

Suh, S., Choi, K.-O., Yang, S.-C., et al. Adsorption mechanism of alkyl polyglucoside (APG) on calcite nanoparticles in aqueous medium at varying pH. Journal of Solid State Chemistry, 2017, 251: 122-130.

Suresh, R., Kuznetsov, O., Agrawal, D., et al. Reduction of surfactant adsorption in porous media using silica nanoparticles. Paper OTC 28879 Presented at Offshore Technology Conference, Houston, Texas, USA, 30 April-3 May, 2018.

Tripathi, R., Alcorn, Z. P., Graue, A. et al. Combination of non-ionic and cationic surfatants in generating CO_2 foam for enhanced oil recovery and carbon storage. Advances in Geo-Energy Research, 2024, 13(1): 42-55.

Wang, Y., Hou, J., Qi, Z., et al. Investigation of sacrificial agents for reducing surfactant adsorption on carbonates. Petroleum Science and Technology, 2022, 40(22): 2755-2772.

Wei, P., Li, J., Xie, Y., et al. Alkyl polyglucosides for potential application in oil recovery process: Adsorption behavior in sandstones under high temperature and salinity. Journal of Petroleum Science and Engineering, 2020, 189: 107057.

Wu, Y., Chen, W., Dai, C., et al. Reducing surfactant adsorption on rock by silica nanoparticles for enhanced oil recovery. Journal of Petroleum Science and Engineering, 2017, 153: 283-287.

Xu, Z., Li, S., Li, B., et al. A review of development methods and enhanced oil recovery technologies for carbonate reservoirs. Petroleum Science, 2020, 17(4): 990-1013.

Yan, H., Guo, X., Yuan, S., et al. Molecular dynamics study of the effect of calcium ions on the monolayer of SDC and SDSn surfactants at the vapour/liquid interface. Langmuir, 2011, 27(10): 5762-5771.

Yekeen, N., Manan, M. A., Idris, A. K., et al. Experimental investigation of minimization in surfactant adsorption and improvement in surfactant-foam stability in presence of silicon dioxide and aluminum oxide nanoparticles. Journal of Petroleum Science and Engineering, 2017, 159: 115-134.

Yu, H., Xue, C., Qin, Y., et al. Preparation and performance of green targeted microcapsules encapsulating surfactants. Colloids and Surfaces A: Physicochemical and Engineering Aspects, 2021, 623: 126733.

Zargartalebi, M., Barati, N., Kharrat, R. Influences of hydrophilic and hydrophobic silica nanoparticles on anionic surfactant properties: Interfacial and adsorption behaviors. Journal of Petroleum Science and Engineering, 2014, 119: 36-43.

Zhang, B., Yang, C., Liao, S., et al. Progress on the synthesis and applications of the green non-ionic surfactant alkyl polyglycosides. RSC Advances, 2025, 15(55): 47333-47359.

Zhang, J., Nguyen, Q. P., Flaaten, A. K., et al. Mechanisms of enhanced natural imbibition with novel chemicals. SPE Reservoir Evaluation & Engineering, 2009, 12: 912-920.

Zhang, R., Somasundaran, P. Advances in adsorption of surfactants and their mixtures at solid/solution interfaces. Advances in Colloid and Interface Science, 2006, 123: 213-229.

Zhong, X., Li, C., Pu, H., et al. Increased nonionic surfactant efficiency in oil recovery by integrating with hydrophilic silica nanoparticle. Energy & Fuels, 2019, 33(9): 8522-8529.

Zhou, W., Dong, M., Liu, Q., et al. Experimental investigation of surfactant adsorption on sand and oil-water interface in heavy oil/water/sand systems. Paper PETSOC-2005-192 Presented at Canadian International Petroleum Conference, Calgary, Canada, 7-9 June, 2005.